DING DEHONG
CUI DAIJUN
and
LI LING

A calibration method based on dual quadratic fitting and nine parameters for mining non-cooled infrared thermal imager

Infrared detection method is mainly used to detect infrared energy field, through which the spontaneous combustion zone of coal can be comprehensively judged. In order to ensure the accuracy of the temperature of the test target under the mine, the paper mainly studies the calibration method of the uncooled infrared imager under the influence of the environment temperature, distance, the effect of the working temperature of the detector and the other factors. A new method of calibration model of dual quadratic fitting and the calibration equation of nine parameters method are proposed. Compared to existing methods, the proposed method is used to process the experiment, and it is concluded that the average error is within 1ºC, which can meet the requirements of temperature measurement-thermal imaging under the mine.

Keywords: *Mining non-cooled infrared thermal imager, dual quadratic fitting, nine parameters, calibration steps, downhole temperature, anomalous region.*

1. Introduction

At present, the research and quotation mainly focus on the defects detection of building materials in civil engineering, quality inspection of building exterior wall construction, forest fire prevention, fire extinguishing, remote sensing resources investigation and so on [1-2]. The infrared detection technology is applied to the coal industry later [3], and the coal industry is limited to the infrared thermometer with spot temperature measurement [4]. The application of infrared imager in coal mine is in the initial stage [5]. Due to the maturity of infrared technology and the continuous development of infrared imager, the infrared imager has the advantages of high sensitivity and surface temperature measurement [6], which will make it a new trend to use infrared imager to detect the abnormal temperature area under the mine.

Mr. Ding Dehong, College of Electrical and Information Engineering, Hunan University, Changsha 410 082, Ding Dehong and Ms. Li Ling, Hunan Province Cooperative Innovation Center for The Construction & Development of Dongting Lake Ecological Economic Zone, Hunan University of Arts and Science, Changde 415 000 and Mr. Cui Daijun, Eado Monitoring Technology Co., Ltd., Zhuhai 519 085, China

The infrared detection method is simple, rapid and accurate. It is the high and new technology equipment in the field of detection at present, which is the development direction of the coal spontaneous combustion high temperature fire source area detection. The instruments are mainly used in infrared detectors and infrared imagers. In China, infrared detectors and infrared imagers are mainly used in coalfield geological survey, geological structure judgment, earthquake prediction, groundwater detection, rock burst and so on [7-8]. Infrared detectors and imagers are used to detect the spontaneous combustion temperature and position of coal walls and pillars in the United States [9]. In some mining areas, good results have been achieved [10]. However, the infrared thermometer can only realize the point monitoring of infrared energy. In order to accurately determine the range of the fire area, many measuring points need to be arranged, and it is difficult to determine the temperature and depth of the fire area for a long time. According to the present research situation, infrared imager is used to realize the two-dimensional monitoring of infrared energy field, to detect the position, range and spontaneous combustion temperature of coal pillar.

Alleged calibration uses standard black-body radiation source of infrared thermometer measurement result correction work to obtain the thermal imager digital output[11].The research shows that the actual temperature, the temperature measuring system and the measured radiation source of the unknown target radiation source must be in the same environment in the calibration process[12]. The instrument is calibrated at the same distance so that the actual radiation temperature of the target can be plotted. The infrared thermograph with weighted least squares correction model based on weighted least square method and least square method is used to calibrate the experiment and radiation measurement, which has a strong practical value and a certain reference significance. The infrared calibration system is of high accuracy and is simple and easy to use[13], which is applicable to the measurement and calibration of target infrared radiation characteristics. Some scholars use support vector machine (SVM) fitting to get the environment temperature and the machine core temperature error correction

model by using the modified method compared to the calibration of the high precision thermocouple temperature measurement, which can make the measurement distance 2m at the time of the temperature measurement error reduced by 50%.

This paper proposes a new method for calibration model, dual quadratic fitting, and nine parameters calibration equation.The method of using the remote small source method for measuring scale experiment and get the error is within ±1□, which can meet the requirements of temperature and thermal imaging. It can also work well at room temperature. Therefore, the first presentation of the basic theory of infrared thermal image calibration fitting relationship between temperature and gray, and the determination of fitting equation, and then discuss in detail the design of the infrared thermal image instrument calibration and the experimental steps and methods.

2. Selection of infrared imager for mine

The radiant energy of the measured object must pass through the atmosphere to reach the instrument, so it is very important to select the working band of the instrument correctly. There are 3 infrared air windows in the ground atmosphere, that is 1-2.5μm, 3-5μm, 8-13μm, but the underground mine infrared radiation is scattered by different gases, coal dust particles and so on. The fluctuation of radiation rate makes the intensity of light seriously attenuate and instability, and has a direct impact on the accurate measurement of temperature. The wavelength in the 2.7-3.2 μm *m* section is the most unsuitable for use. In addition, there are water vapour, carbon dioxide, methane and other gases in the downhole air. All these gases have one or several absorption peaks. Therefore, a variety of factors must be taken into consideration when selecting the working band. After weighing, it is considered that if the measuring distance exceeds 8m, under the condition of heading and mining face, 3.5-6.0μm band should be adopted. If the measuring distance is less than 5m, 8-14μm band can be selected.

3. The modelling of calibration

Target (bold) temperature detector and output relation curve of "S" type curve, as is shown in Fig.1. Due to thermal imaging system a saturation point receiving thermal radiation is the independent variable in high and low temperature respectively, and infrared image gray scale *D* is a dependent variable, so that it will be used in fitting curve black-body temperature *T* as independent variables, when the temperature is calculated according to the fitted curve equation and image gray value.

The temperature calibration process must be the independent variable of the target temperature before the temperature has a gray degree, and the coefficients of the quadratic polynomials are fitted, and the calculation

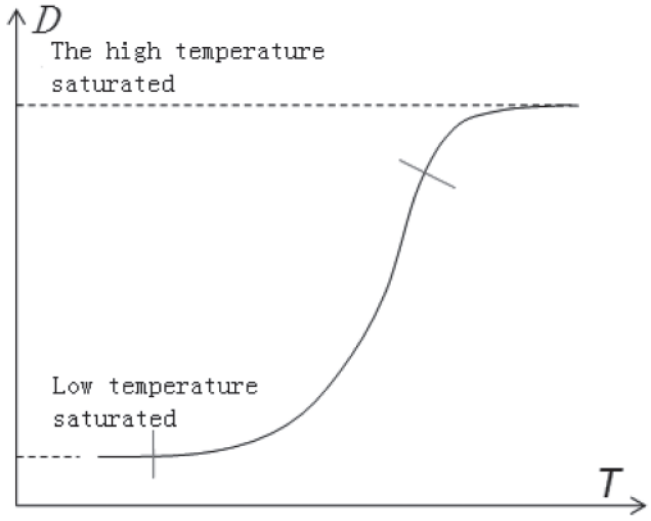

Fig.1 The relationship between the gray degree of thermal image and temperature

temperature is calculated according to the quadratic polynomial. The calibration equation is

$$D_0 = a + b * T + C * T^2 \quad \text{... (1)}$$

When the temperature is measured, the gray degree is obtained, and the temperature is calculated.

$$T(D_0) = \frac{-b + \sqrt{b^2 - 4c(a - D_0)}}{2c} \quad \text{... (2)}$$

The fitting equation is determined by considering the fitting degree, extrapolation effect and calculation quantity.

The polynomial fitting is

$$D(T) = a + b * T + c * T^2 + \ldots \quad \text{... (3)}$$

The exponential function fitting is

$$D(T) = \exp(a * T + b) \quad \text{... (4)}$$

The logistic function is

$$D(T) = \frac{a}{b * \exp\left(\frac{1}{T}\right) - 1} \quad \text{... (5)}$$

The compertz function fitting is

$$D(T) = a * b^{C^T} \quad \text{... (6)}$$

Detector temperature does not change the calibration curve of function types, tensile and translation only in the calibration curve function parameters *a*, *b*, *c* is a function of the detector temperature *Tt* and coefficient and detector temperature relationship is drab, and the relationship can be determined through experiments.

$$a = Fa(Tt),\ b = Fb(Tt),\ c = Fc(Tt) \quad \text{... (7)}$$

According to the probe temperature *Tt*, the values of *a*, *b* and *c* are obtained, and the target temperature *D* is obtained

according to the calibration fitting function and the gray value *T*.

The terrestrial phoenix has been described reasonably well, and the ideal radiation calibration model of the detector is proposed.

$$N_{AD} = K_1 L_S(T) + C_1 \quad \text{... (8)}$$

In the formula, $L_S(T)$ is the standard black body source radiation brightness, K_1 is the fixed parameter of the detector, C_1 is the constant term. This section proposes a new calibration model – double quadratic fitting, and 9 parametric calibration equations, which are compared to the existing methods, and the performance of the calibration tests is measured.

4. Calibration steps

The whole calibration process is carried out in the chamber of constant temperature and humidity test chamber, and the indoor size of 4m*4m*2m is used to set up a ring platform in the room, which can be evenly placed in multiple black bodies T_1, T_2, T_3 and so on , room center has a rotational platform, it corresponds to place multiple thermal imager black-body □, □, □, and so on. Each thermograph is allowed to collect a black body image. Adjust the temperature and humidity of room and complete the calibration of the detector's temperature drift. The distance between the thermal imager and the black-body is 1m. The control of data acquisition and rotary table is carried out in the calibration room.

Scanning the probe wide temperature segment, the relationship curve is divided according to the saturation trend of gray value. The temperature of the detector was scanned, and the temperature of different ambient temperature was determined. Because of the difference between the detectors, the temperature and temperature of the black body must be scanned and the best temperature points are obtained.

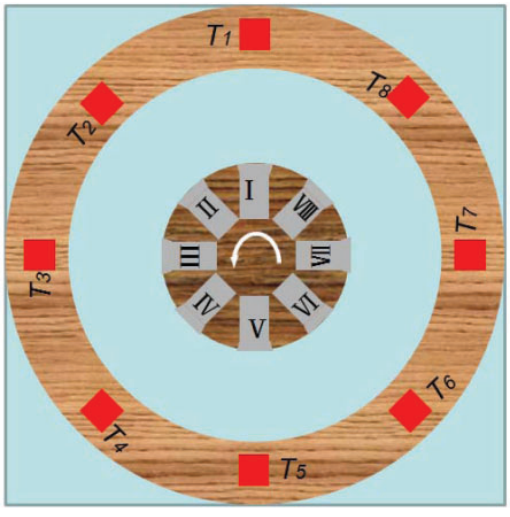

Fig.2 The schematic diagram of the internal structure of calibration room

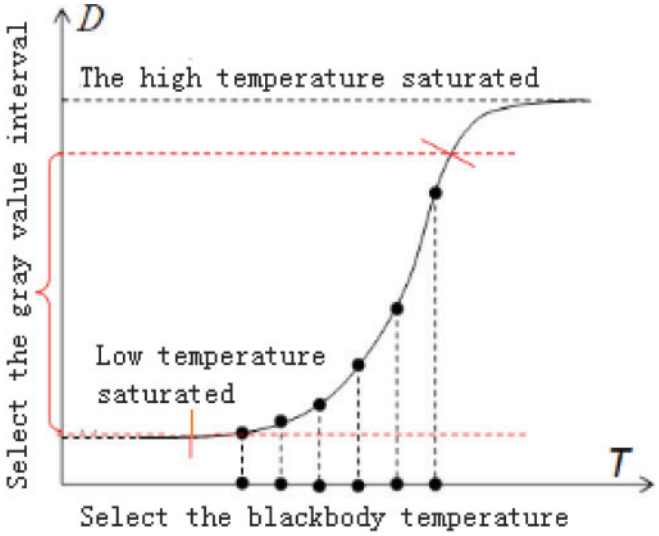

Fig.3 The calibration temperature point selection and gray level selection schematic

To1 set into the chamber temperature, environment temperature and detector temperature stabilized, intermittent rotation rotating platform, according to the following table by computer control each thermal imager to collect a series of black body image, at the same time record *Tt*1 detector temperature. The number of thermal imagers is less than or equal to the number of black-bodies. After the collection, set the temperature *To*2 in the chamber, and the temperature of the series black body, and also collect a series of black body images. According to the preliminary experimental results and the application environment of thermal imager, the data of several environmental temperature points are *To*1, *To*2, *To*3, and so on. Corresponding probe temperature point: *Tt*1, *Tt*2, *Tt*3, and so on. The collecting the black body image data is shown in Table 1.

The relationship between the final detector temperature *Tt*, black body temperature *T* and image grayscale *D* can be expressed by the calibration model

$$D = FD(T, Fa(Tt), Fb(Tt), Fc(Tt)) \quad \text{... (9)}$$

The inverse function of *D* can get the true temperature

$$T = FT(D, Tt) \quad \text{... (10)}$$

The temperature is the independent variable and the quadratic function is fitted to the temperature curve. A quadratic function (calibration equation) is fitted for each detector temperature t_x.

$$D = Fa(t_x) * T^2 + Fb(t_x) * T + Fc(t_x) \quad \text{... (11)}$$

Among them, *D* is the infrared image grayscale, *T* is the black body temperature, $Fa(t_x)$, $Fb(t_x)$, $Fc(t_x)$ is the coefficient, each coefficient is the function of detector temperature t_x. The function of the coefficients is fitted according to the relationship between the coefficients and the temperature of the detector.

TABLE 1: THE COLLECTING THE BLACK BODY IMAGE DATA

Thermal imager	□	□	□	□	□	□	□	□
Black-body acquisition								
1	T1	T2	T3	T4	T5	T6	T7	T8
2	T2	T3	T4	T5	T6	T7	T8	T1
3	T3	T4	T5	T6	T7	T8	T1	T2
4	T4	T5	T6	T7	T8	T1	T2	T3
5	T5	T6	T7	T8	T1	T2	T3	T4
6	T6	T7	T8	T1	T2	T3	T4	T5
7	T7	T8	T1	T2	T3	T4	T5	T6
8	T8	T1	T2	T3	T4	T5	T6	T7

TABLE 2: THE RELEVANT TEMPERATURE POINTS WITH CORRESPONDING DETECTOR TEMPERATURE PARAMETERS

Temperature points collected	3ºC	13ºC	13.3ºC	24.8ºC	28.6ºC	29.6ºC	36.7ºC	49.5ºC
Corresponding detector temperature parameters	8666	9097	9110	9625	9816	9840	10045	10555

The calibration process obtains nine data A_2, A_1, A_0; B_2, B_1, B_0; C_2, C_1, C_0. When temperature measurement, the coefficients of the current calibration equation are obtained by the temperature parameters of the detector.

$$F_a = A_2 * t_x^2 + A_1 t_x + A_0$$
$$F_b = B_2 * t_x^2 + B_1 t_x + B_0 \quad \ldots (12)$$
$$F_c = C_2 * t_x^2 + C_1 t_x + C_0$$

The coefficients of the calibrated fitting equation $Fa(t_x)$, $Fb(t_x)$, $Fc(t_x)$ are calculated according to the detector temperature. According to the image grayscale D_0 and the calibration fit equation, the target temperature is calculated.

$$T(D_0) = \frac{-F_b(t_x) + \sqrt{F_b(t_x)^2 - 4 * F_a(t_x) * (F_c(t_x) - D_0)}}{2 * F_a(t_x)} \quad \ldots (13)$$

5. Experimental results

Low temperature environment acquisition: the thermal imager is energized, the sealing box is put into the cooler whole, and the temperature is stable and then removed. Due to the isolation of the sealed box, the environment in the pit of the short time internal thermal imager will not change abruptly, and there is enough time to collect the black body image. The heat exchange process of the laboratory is slow, the environment in the sealed box is relatively stable, and the black body image can be collected during the heating process. The germanium chip has a condensation fog at low temperature, and the image is collected after using the mirror paper to wipe the water mist.

High temperature environment acquisition: the thermal imager can be charged, the sealing box is in the high temperature box, and the black body image is collected after stabilization.Temperature of normal temperature: set the air conditioning temperature of calibration room.The relevant temperature points with corresponding detector temperature parameters is shown in Table 2.

After the probe electric stability, assume that the probe has a linear relation and the environment temperature, the temperature parameters in the subsequent fitting and measuring parameters of temperature measuring probe with the detector temperature drift caused by the environmental temperature under the mine.

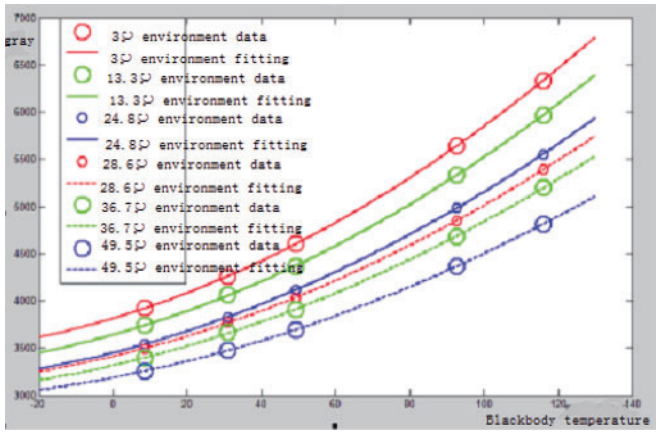

Fig.4 The temperature measurement curve in different environment

Select 3 □, 13.3 □, 24.8 □ and 28.6 □, 36.7 □ and 49.5 □ environment in the pit, its image grey-black body temperature data fitting curve calibration equation is indicated in Fig.4.

As shown in Fig.4, the calibration fitting equation with the detector temperature variation regularity is stronger and it is concluded that the detector temperature calibration fits the equation coefficient.

In this paper, the effect of a linear fitting is applied to the temperature drift equation of each coefficient, and the coefficients of the quadratic fitting temperature drift equation are determined. Take different temperature points of the environment to fit the calibration curve and test the temperature under the mine.

EXPERIMENT 1

The ambient temperature are 3ºC, 24.8ºC, 36.7ºC and 49.3ºC. The calibration is finished in this condition by the

Table 3: The results of experiment 1

The detector: 9098	Blackbody temperature	8.5	31	49.2	92.6	116	Average: 0.4184
Environment: 13□	Calculating temperature	8.0229	30.717	49.054	92.5153	116.5171	
	Error	0.4771	0.283	0.146	0.0847	0.5171	
	Average error: 0.3016						
The detector: 9840	Blackbody temperature	8.5	31	49.2	92.6	116	
Environment: 29.6□	Calculating temperature	9.1176	31.4375	48.4244	92.22	115.5353	
	Error	0.6176	0.4375	0.7756	0.38	0.4647	
	Average error: 0.5351						

Table 4: The results of experiment 2

The detector: 9098	Blackbody temperature	8.5	31	49.2	92.6	116	Average: 1.0216
Environment: 13□	Calculating temperature	7.7079	30.4361	48.7354	91.9955	115.8497	
	Error	0.7921	0.5639	0.4646	0.6045	0.1503	
	Average error: 0.5151						
The detector: 9840	Blackbody temperature	8.5	31	49.2	92.6	116	
Environment: 29.6□	Calculating temperature	8.9911	31.3216	48.2931	92.0021	115.2561	
	Error	0.4911	0.3216	0.9069	0.5979	0.7439	
	Average error: 0.6123						
The detector: 10555	Blackbody temperature	8.5	31	49.2	92.6	116	
Environment: 49.5□	Calculating temperature	9.7841	32.4586	50.4025	95.2048	119.1366	
	Error	1.2841	1.4586	1.2025	2.6048	3.1366	
	Average error: 1.9373						

calibration curve. The temperature measurement point are 13ºC and 29.6ºC. The calculated temperature measurement results under the mine by calibration curve which can be seen in Table 3.

Experiment 2

The ambient temperature are 3ºC, 24.8ºC and 36.7ºC. The temperature measurement point are 13ºC, 29.6ºC and 49.5ºC. The calculated temperature measurement results under the mine can be seen in Table 4.

The experiment result shows that the average error within 1 □ by using the solution and calibration equation, which can meet the requirements of temperature and thermal imaging in the pit. The smaller the detector's temperature is, the higher the accuracy is, it should be possible to work under normal temperatureunder the mine.

4. Conclusion

In the calibration experiment, both the black body temperature and the detector temperature are the independent variables, and the calibration equation and the coefficient temperature drift equation should be fitted with quadratic function. The number of black-bodies should be 5 or 6, and at least four environmental temperature points should be specified, and the temperature range should be wide. Example: <5ºC, 20ºC, 35ºC, >50ºC. Through a series of experiments to get the average error within 1 □, it can satisfy the engineering requirement of thermal imaging temperature measurement.

Acknowledgement

This work is supported by Hunan province key high-tech project (Grant No. 2016GK2019). The general project of Hunan province department of education (Grant No.16C1089), and Dr. Launch funds of the scientific research of Hunan University of Arts and Science.

References

1. Zhang, Xiao-long and Liu, Ying (2012): "Radiation calibration of high-precision andnon-cooled long wave infrared thermal imager." *China Optical*, 2012, 5(3):63-74.
2. Li, Yun-hong and Zhang, Long (2010): "Second calibration of the Infrared temperature measurement in field atmospheric transmittance." *Optical Precision Engineering*, 2010, 18(10):21-43.
3. Song, Xiao-mei and Zhou, Kang-kang (2015): "The calibration of infrared thermal imager based onminimum weight." *Infrared*, 2015, 11(5):101-110.
4. Jiang, Guo-wei and Li, Cheng-long (2015): "A calibration of infrared thermal imager method based on trinocular vision." *Computer Applications and Software*, 2015, 6(1):55-64.
5. Li, Bin and Wu, Hai-ying (2014): "A design of simple Infrared calibration system." *Infrared and Laser Engineering*, 2014, 43(2):458-463.
6. Hao, Ji-ping and Du, Cheng-gong (2014): "Oretical

calculation and response of infrared calibration." *Applied Optics*, 2014, 25(2):36-39.

7. Yuan, Yu-kai (2017): "Method for eliminating stray light in optical system." *Journal of Atmospheric and Environmental Optics*, 2017, 22(11):102-113.
8. Hao, Yun-cai and Xiao, Shu-qin (2015): "Status and development of stray light technology for spaceborne optical remote sensor." *Space Science and Technology*, 2015, 17(3):40-50.
9. Hu, Gui-hong and Chen, Qian (2013): "Infrared focal plane detector nonlinear response determination." *Photoelectron Laser*, 2013, 14(5):489-492.
10. Sun, Xue-jin and Liu, Jian (2008): "The radiation of the uncooled infrared focal plane array calibration model." *Journal of PLA University of Technology*, 2008, 9(4):399-403.
11. Hu, Xu-xiao and Pan, Xiao-hong (2010): "A multi order exponential function recursive fitting algorithm." *Journal of Zhejiang University*, 2010, 44(12):99-108.
12. Lv, Shou-peng and Pan, Yuan-yuan (2012): "Method of measuring Planck constant in photoelectric effect and thermal effect of Fitting Correcting common figure." *Science and Technology and Engineering*, 2012, 12(13):56-63.
13. Zhang, Xiaoye and Xu, Chao (2016): "Temperature field of body surface measurement by uncooled infrared thermal imager and error correction." *Infrared and Laser Engineering*. 2016, 45(10):38-44.

UAV APPLICATIONS ON PROJECTS MONITORING IN MINING AND CIVIL ENGINEERING

(Continued from page 872)

6. Liu, X., Chen, P., Tong, X., Liu, S., Liu, S., Hong, Z., Li, L. and Luan, K. (2012 June): UAV-based low-altitude aerial photogrammetric application in mine areas measurement. In Earth Observation and Remote Sensing Applications (EORSA), 2012 Second International Workshop on (pp. 240-242). IEEE.
7. González-Aguilera, D., Fernández-Hernández, J., Mancera-Taboada, J., Rodriguez-Gonzálvez, P., Hernández-López, D., Felipe-García, B., Gozalo-Sanz, I. and Arias-Perez, B. (2012): "3D modelling and accuracy assessment of Granite Quarry using unmanned aerial vehicle." *ISPRS Ann. Photogram. Remote Sens. Spat. Inf. Sci*, 1, pp.37-42.
8. Draeyer, B. and Strecha, C. White paper: how accurate are UAV surveying methods? Pix4D, 14. https://support.pix4d.com/entries/40219303-How-accurate-are-UAV-surveying-methods?
9. Mmcuav- Multi micrometer UAV Aero Technology Pvt Ltd- www.mmcuav.com
10. Nex, F. and Remondino, F. (2014): "UAV for 3D mapping applications: a review." *Applied Geomatics*, 6(1), pp.1-15.
11. Patikova, A. (2004): "Digital photogrammetry in the practice of open pit mining." *Int. Arch. Photogramm. Remote Sens. Spat. Inf. Sci* 34 (2004): 1-4.

Printed by Pradip Kumar Chanda at The Indian Press Pvt. Ltd. 93A Lenin Sarani, Kolkata 700 013 and published by him for Books & Journals Pvt. Ltd. from 6/2 Madan Street, Kolkata 700 072.